Preliminary Investigation of Helicon Plasma Source for Electric Propulsion Applications

Kyoichiro Toki,[*1] Shunjiro Shinohara,[*2] Takao Tanikawa,[*3] Ikkho Funaki[*4] and Konstantin P. Shamrai[*5]

*1 Institute of Space and Astronautical Science
3-1-1 Yoshinodai, Sagamihara, Kanagawa 229-8510, Japan
Phone : +81-42-759-8285 FAX : +81-42-759-8462
E-mail : toki@newslan.isas.ac.jp
*2 Interdisciplinary Graduate School of Engineering Sciences,
Kyushu University, 6-1 Kasuga-Koen, Kausga, Fukuoka 816-8580, Japan
Phone : +81-92-583-7649 FAX : +81-92-571-8894
E-mail : sinohara@aees.kyushu-u.ac.jp
*3 Research Institute of Science and Technology, Tokai University,
2-28-4 Tomigaya, Shibuya-ku, Tokyo 151-0063, Japan
Phone : +81-3-3467-2211, ext. 472 FAX : +81-3-3467-6177
E-mail : tnth@keyaki.cc.u-tokai.ac.jp
*4 Institute of Engineering Mechanics and Systems, University of Tsukuba,
1-1-1, Ten-nodai, Tsukuba, Ibraki 305-8577, Japan
Phone : +81- 298-53-5130 FAX : +81- 298-53-5207
E-mail : funaki@kz.tsukuba.ac.jp
*5 Scientific Center Institute for Nuclear Research, National Academy of Sciences,
47 Prospeckt Nauki, Kiev 28, 03680 MSP, Ukraine
Phone : +380-44-2652616 FAX: +380-44-2654463
E-mail: kshamrai@kinr.kiev.ua

Abstract

A new concept of electrodeless discharge and electromagnetic acceleration for next generation electric propulsion has been proposed. A preliminary investigation was conducted for a newly designed very small helicon plasma source of 2.5 cm i.d. with 4.7 cm long confined geometry and 15 cm long open configuration using glass tubes. The RF frequency was selected between 40 – 60 MHz ignitable for both configurations with less than and equal to 50 W input power. For both configurations, plasmas were successfully initiated and stably maintained. The plasma density was found to be 10^9 – 10^{12} cm^{-3} for Ar propellant of 0.8 – 20 mg/s flow rates and applied magnetic fields of 0 – 300 G. These plasma features showed good qualitative accordance with theoretical predictions using a parallel antenna and are promising for future evolution to higher density.

1. Introduction

Helicon plasma sources have been paid keen attention worldwide. This type of plasma source has versatile applications to various cylindrical plasma sources with diameters typically from 5 cm to 15 cm or much larger diameters for plasma physics research up to 75 cm i.d (73.8 cm o.d.). (Fig. 1) using various antennae.[1-6] The available plasma density can reach 10^{13} cm^{-3} being equivalent to or exceeding ECR plasmas. The helicon wave is so-called a whistler wave or R-wave under the existence of magnetic fields, and the application frequency is in the following ω range, where ω_{ci} is ion cyclotron frequency and ω_{ce} is electron cyclotron frequency.

$$\omega_{ci} << \omega << \omega_{ce} \qquad (1)$$

Since the plasma production process does not require resonant condition, the choice of RF frequency and applied magnetic field strength are flexible parameters from MHz until microwave frequency, and from 30

over 1,000 G, respectively. The absorption mechanism of helicon wave was so far believed Landau damping but has been pointed out that the process is well explained by the mode transformation from helicon to Trivelpiece-Gould wave.[7]

Now there are some helicon sources in the field of next-generation electric propulsions with electrodeless configuration such as VASIMR (Variable Specific Impulse Magnetoplasma Rocket)[8] M2P2 (Mini-Magnetospheric Plasma Prorpulsion)[9], helicon ion thruster,[10] and other smaller plasma sources.[11] These plasma sources are based on electrodeless plasma production, however, the VASIMR uses magnetic nozzle acceleration dependent on ICRH (Ion Cyclotron Resonance Heating) while the helicon plasma source uses non-resonant process, the M2P2 is not a thruster itself, and the helicon ion thruster employs gridded electrostatic accelerations inherently erodible.

In this paper, we propose a new application concept of helicon plasma source to the next generation-electric propulsion having no erodible discharge electrodes for either plasma production or plasma acceleration and also being free from resonance conditions that fix a usable RF frequency or a magnetic field strength. This is one of the world smallest helicon plasma source, while the world largest helicon plasma source of 73.8 cm i.d.(75 cm o.d.) vacuum chamber is in operation in our group (Fig. 2).[3,4]

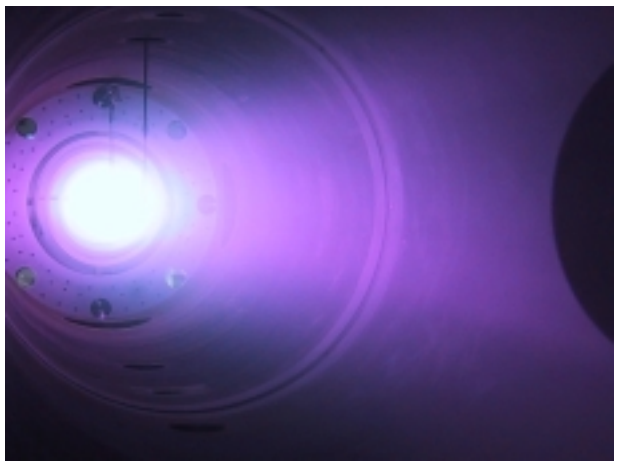

Fig. 1 73.8 cm i.d.(75 cm o.d.)chamber large helicon plasma source run in ISAS by Shinohara and Tanikawa.[3,4]

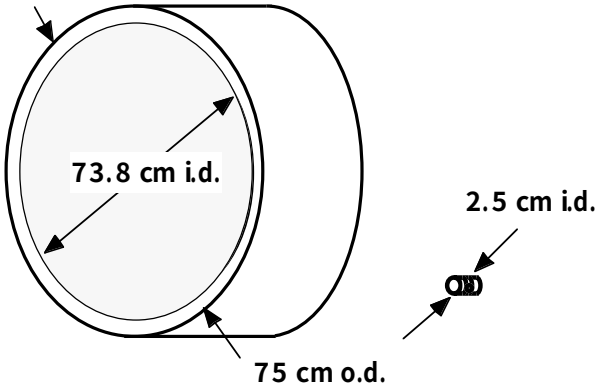

Fig. 2 From very large to very small helicon plasma sources to be prepared.

2. A New Concept of Helicon Plasma Thruster

2.1 Small Helicon Plasma Source

In this study, two types of helicon plasma sources are investigated. One is a confined plasma source having metallic bulkheads in both ends of a short cylindrical glass tube as described later. Another is an open plasma source in the down stream direction as shown in Fig. 3. This provides a new concept of electromagnetic acceleration thruster without cathodes nor anodes using a helicon plasma source. This thruster is very small in size, 2.5 cm i.d. for plasma production region and about 15 cm in length including plasma acceleration zone. In the plasma production zone, a popular helicon source configuration is employed with a glass tube and an upstream end-plate having a propellant port. This has a magnetic coil to apply an axial field to the plasma production zone and a diverging field to the plasma acceleration zone.

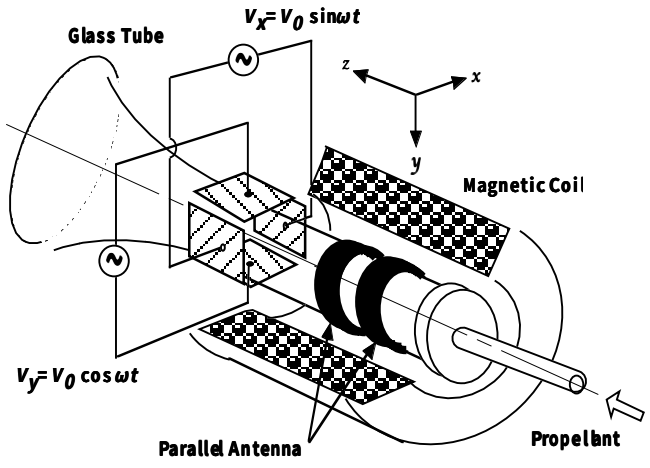

Fig. 3 Concept of rotating electric field "Lissajous" acceleration of plasma (a sort of electrodeless MPD thruster) with helicon plasma source.

2.2 "Lissajous" Acceleration, An Electrodeless MPD Thruster Concept

The peculiar portion of this device is two pairs of parallel plates applying sinusoidal electric fields with 90 degrees phase difference so that the plasma in the acceleration zone is rotated in azimuth direction just like a "Lissajous" figure of the cathode ray in a CRT. As shown in Fig. 4, the plasma equation of motion in this "Lissajous" acceleration is expressed as following equations.

$$m\frac{du_x}{dt} = eE_x - m\nu u_x + eu_y B_z \qquad (2)$$

$$m\frac{du_y}{dt} = eE_y - m\nu u_y - eu_x B_z \qquad (3)$$

Here, t : time, m : ion or electron mass, e : electronic charge, ν : collision frequency, B : applied magnetic field strength, u : ion or electron velocity, E : applied electric field, $\omega_0 = eB/m$, x, y ,z : Coordinates depicted in Fig. 3. The solution of these differential equations includes a general solution decaying exponentially by $-\nu t$ and a valid special solution finally remained below.

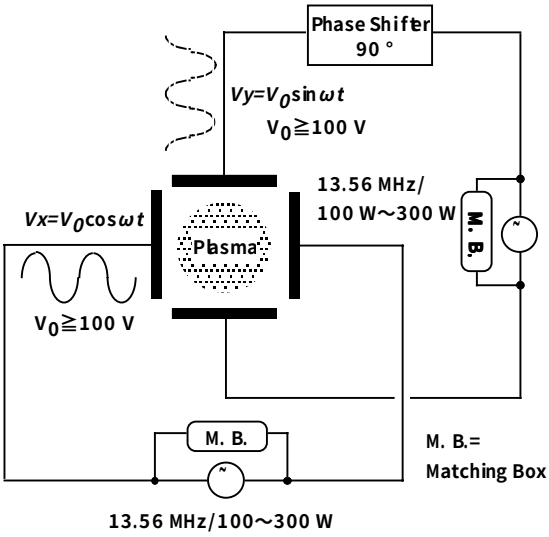

Fig. 4 Rotating electric fields in x and y Direction for "Lissajous" acceleration of plasma.

$$u_x = \frac{eE_0}{m}\frac{1}{\sqrt{(\omega_0-\omega)^2+\nu^2}}\sin(\omega t+\phi) \qquad (4)$$

$$u_y = \frac{eE_0}{m}\frac{1}{\sqrt{(\omega_0-\omega)^2+\nu^2}}\cos(\omega t+\phi) \qquad (5)$$

$$\tan\phi = \frac{\omega_0-\omega}{\nu} \qquad (6)$$

$$\nu = \nu_{ela} + \nu_{inela} \qquad (7)$$

$$\delta = \sqrt{\frac{2}{\omega\mu_0\sigma}} \qquad (8)$$

$$R_{L,eq} = \frac{eE_0}{m\omega^2} \qquad (9)$$

Apparently the ions and electrons gain rotational velocity around z-axis and power by rotating applied electric fields of E_x and E_y as long as the collision frequency ν has a finite value. The collision frequency involves elastic ν_{ela} and inelastic ν_{inela} collisions especially charge exchange collisions ν_{cex}. When an appropriate frequency ω, for example 13.56 MHz relatively a low frequency, the skin depth δ (above equation is an approximation of conductive surface) into plasma has an effective depth of deeper than 1 mm where μ_0 is magnetic permeability and this is another reason of small helicon plasma source is selected. The rotating radius of ions and electrons (a sort of equivalent Larmor radii $R_{L,eq}$ determined by rotating electric field) are well in the mm order, if one uses 500 W class RF power supply with expected loading of several tens of volts.

After gaining rotational motion of plasma, that energy is transformed into a rotational momentum

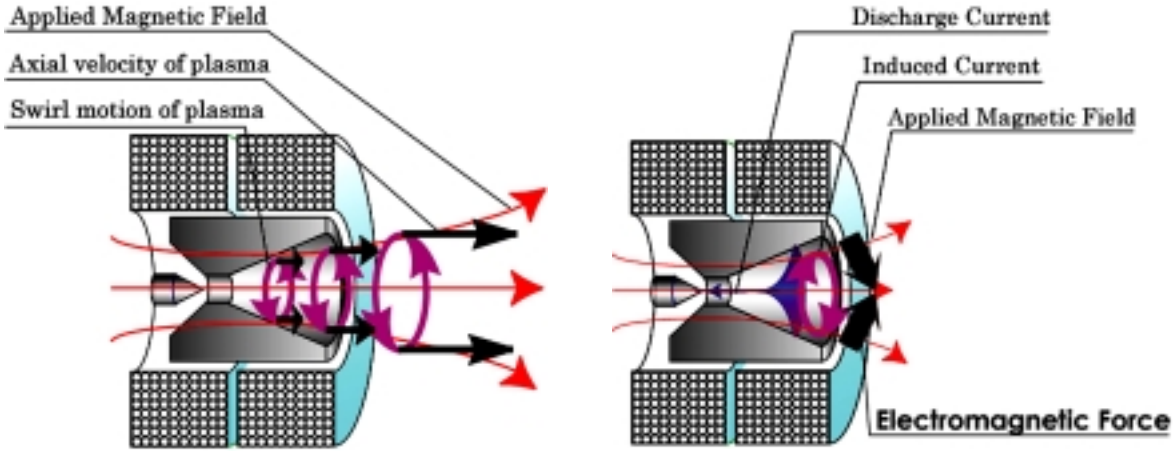

Fig. 5 MPD arcjet acceleration mechanism with the external magnetic field applied (Left: swirl acceleration by transformation of, rotational to translational velocity, Right: azimuth Hall current x radial component of B-field acceleration).[12]

which in turn changed to translation energy through the magnetic expansion by the principle of conservation of magnetic moment, or a more promising process of producing azimuth current interacting with radially expanding magnetic field is expected as a "Hall current accelerator" This magnetic coil is also used for helicon plasma production zone. These acceleration mechanisms resemble the processes utilized in applied-field steady-state MPD thrusters as shown in Fig. 5. In other words, this "Lissajous" acceleration type helicon plasma thruster is a kind of electrodeless MPD thruster.[12,13]

3. Experimental Set-up and Measurement Method

3.1 Design of Tow Types of Small Helicon Sources

There are two types of small helicon sources in this study as the proof-of –concept. Both sources use Pyrex glass tube having dimensions of 2.5 cm i.d. and 3.3 cm o.d. The glass tube has a grounded metal end plate with a propellant inlet port for Ar or other gasese such as N_2+2H_2 and Air, although N_2+2H_2 and Air were just used for ignition characteristics examinations this time. We employed a simple two –loop parallel antenna having a copper strip width of 16 mm, the loop spacing of 8 mm, and the strip thickness of 70 μm as shown in Fig. 6.

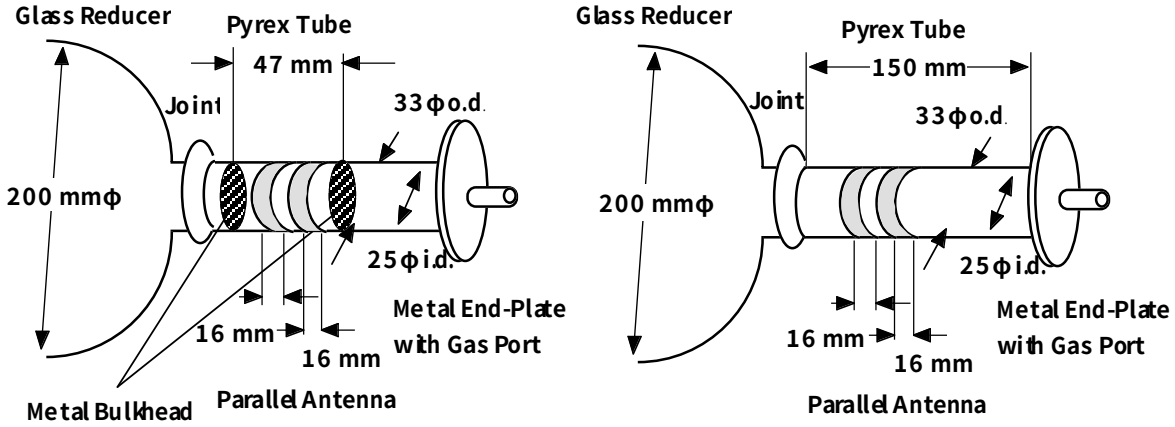

Fig. 6 Two types of small helicon sources used (Left: Short (confined) source, Right: Long (open) source).

Short (Confined) Source

The Short (Confined) source has two grounded metallic bulkheads (1 mm thickness copper plates) inside the tube with a 4.7 cm apart spacing for both positions of upstream and downstream sides of the antenna module. Although the bulkheads confine most of the generated plasma, very small amount of plasmas leaked from the peripheries of these bulkheads and the inner tube wall. This configuration simulates an orificed plasma source to be used small but high-density electron or ion sources and the plasma is evacuated to vacuum chamber via a glass reducer connecting portion.

Long (open) Source

The Long (open) source has an open at the downstream of the glass tube with a 15 cm straight portion with a glass reducer and the two-loop parallel antenna is wound in the midst of the straight portion.

3.2 Experimental Facility and Measurement

The small helicon sources are connected by plastic joints through a Pyrex glass reducer to a metal vacuum chamber of 1.2 m diam. and 2 m length being evacuated by a rotary pump and a mechanical booster pump. The background pressure was less than 1 mTorr for 0.8 mg/s, 37 mTorr for 4 mg/s, 68 mTorr for 20 mg/s flowrate of Ar. A signal generator of Kenwood SG-5150, an RF-amplifier of Thamway T142-4749A with a matching box of Thamway T020-5558A were used for RF power source capable of generating 0 – 100 W at the frequency range of 10 – 100 MHz. A directional coupler inside the matching box monitors the antenna loading of the forward / reflection power and the voltage and current. A solenoid coil of about 400 turns having an i.d. of 11 cm and a length of 14 cm produces 18 gauss/A uniform and almost axial magnetic field at the helicon plasma source. All the experimental set-up is depicted in Fig. 7. A set of floating double probe evaluated the plasma density and temperature. As shown in Fig. 8, a pair of 1 mm diam. tungsten wires were exposed at the tip of 1.5 mm from a 3.4 mm diam. ceramic tube for

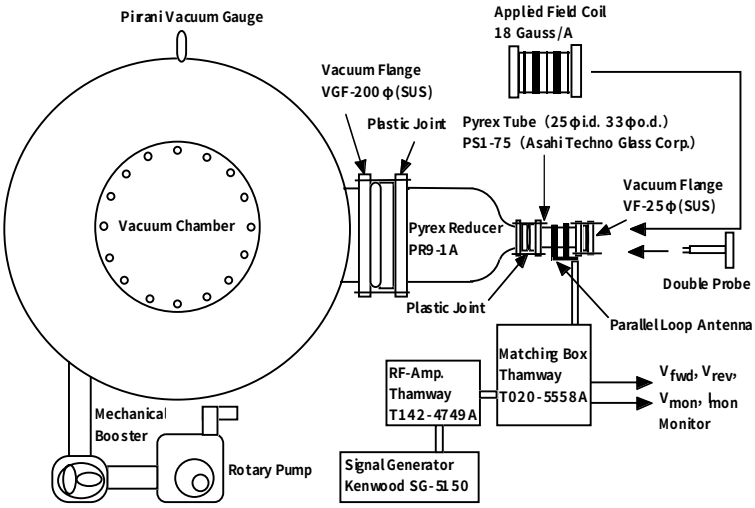

Fig. 7 Experimental set-up.

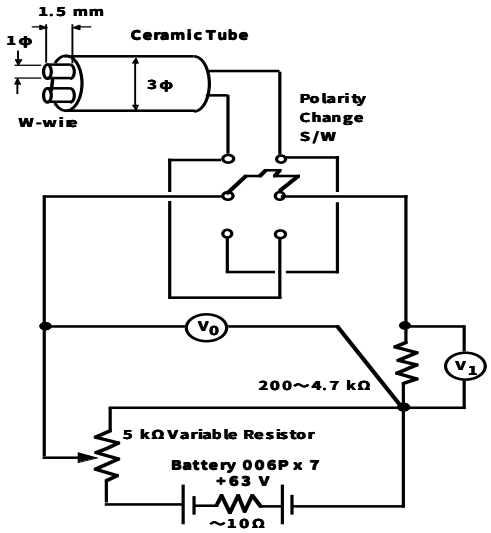

Fig. 8 Double probe measurement circuit.

thermocouple. This probe was inserted to the midst of the helicon plasma sources. The probe biasing voltage and polarity were determined by 63 V layer built batteries with a variable resistor and a toggle switch, respectively to sweep the probe voltage from –63 V to 63 V. The probe voltage and current were read out by electrically floating multimeter.s. As is often recognized in the RF plasmas, the probe curve is skewed except for the ion saturation and very beginning of the electron current portions. Sometimes sophisticated measurements system such as synchronized sweep with the applied RF frequency to trace a single probe curve by using lock-in amplifier and an RF compensation probe are employed, however, in this experiment, the plasma density and temperature were evaluated from the vicinity of ion saturation portion.

4. Experimental Results and Discussion

The first plasma was observed last December as exhibited in Fig. 9 at 60 MHz input for the Long (open) source of Ar flowrate of 4 mg/s. We surveyed ignition characteristics first for both the Short (confined) source and the Long (open) source varying RF frequency from 13.56 MHz to 108.48 MHz at every 13.56 MHz increment. The most appropriate frequencies were found from 40 MHz to 80 MHz where the ignition took place with less than 10 W or sometimes less than 1 W RF input power (Fig. 10).

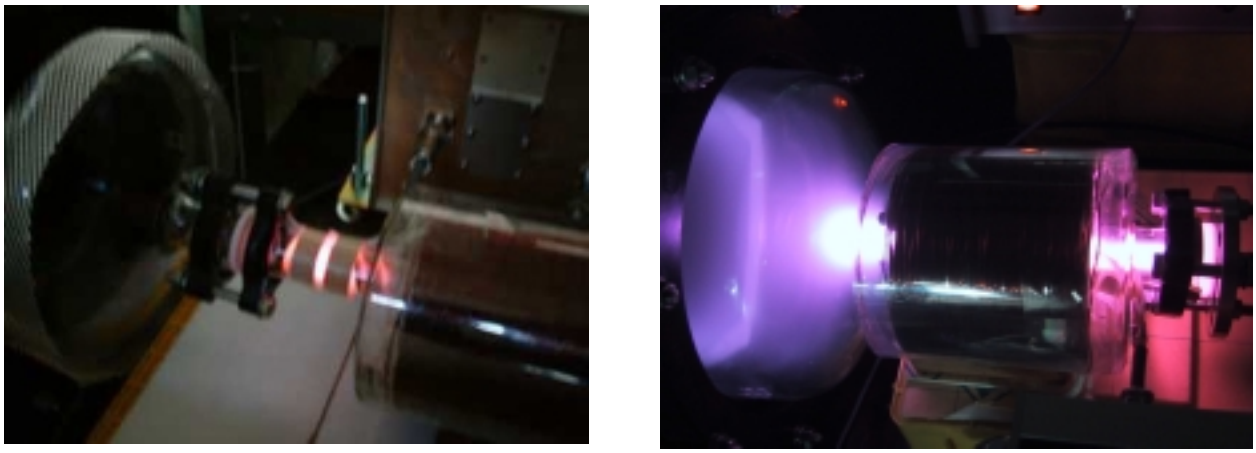

Fig. 9 First plasma of Ar (Left: Short (confined) source, Right: Long (open) source).

In order to determine a main frequency or other operating conditions for both the Short (confined) source and the Long (open) source, under the input RF power range up to 50 W, the frequency dependence was surveyed, the B-field dependence, and the flowrate dependence. For the no applied B-field case, which is no helicon mode, at a flowrate 4 mg/s Ar, the plasma density n_i increased with RF input power from 10^9 cm^{-3} to 10^{10} cm^{-3} with electron temperature Te of 3 eV or dispersed at higher RF input power for the Short

(confined) source and n_i of 10^{11} cm-3 was achieved with relatively low Te of 2-3 eV for Long (open) source (Fig. 11). We selected 40.68 MHz for Short (confined) source, and 54.24 MHz for the Long (open) source because of the highest n_i.

For the various B-fields with a flowrate of 4 mg/s Ar, the Short (confined) source achieved a density increase by two order of magnitudes from 10^9 cm^{-3} to 10^{11} cm^{-3} at a B-field of 300 gauss with Te of 2-4 eV, while the Long (open) source exhibited more rapid n_i increase from 10^{11}cm^{-3} to 10^{12} cm^{-3} with lower Te of 1-2 eV (Fig. 12).

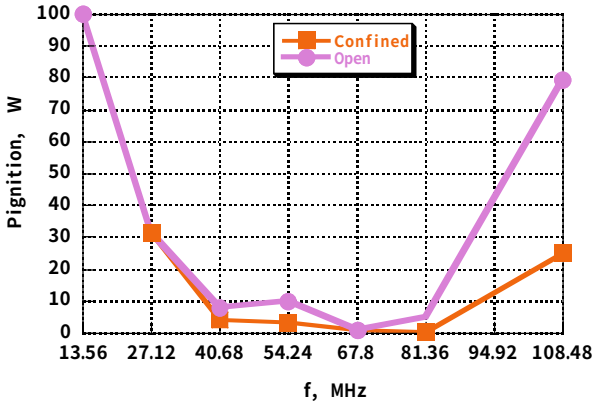

Fig. 10 Ignitable RF power vs. frequency.

For the various Ar flowrates, the Short (confined) source at 100 gauss B-field, only 0.8 mg/s indicated apparent density jump at higher RF input power 25 – 50 W with Te of 2- 4 eV, while the Long (open) source revealed a rapid n_i increase up to 10^{12} cm^{-3} the maximum dens ity in this study with relatively low Te of 1-2 eV (Fig. 13). In all cases the Te at higher power around 50 W was scattered violently 1-6 eV perhaps due to RF effects on the probe even if the very restricted portion of the probe curve around ion saturation was used. The plasma load resistance for both Short (confined) source and the Long (open) source were measured to be 0.1 – 1 Ω from forward and reflected RF powers and antenna V, I loading characteristics, however, the error of this measurement reaches 100 % due to imperfect matching and was discarded.

Usually the RF plasmas are ignited from CCP (Capacitively Coupled Plasma) mode, increase density in ICP (Inductively Coupled Plasma) mode, and make a density jump at helicon mode at a certain input power. The jump condition is a function of both pressure and applied magnetic field. The experimental results of Fig. 11 are obviously in ICP mode because no magnetic field was applied. But the density jump

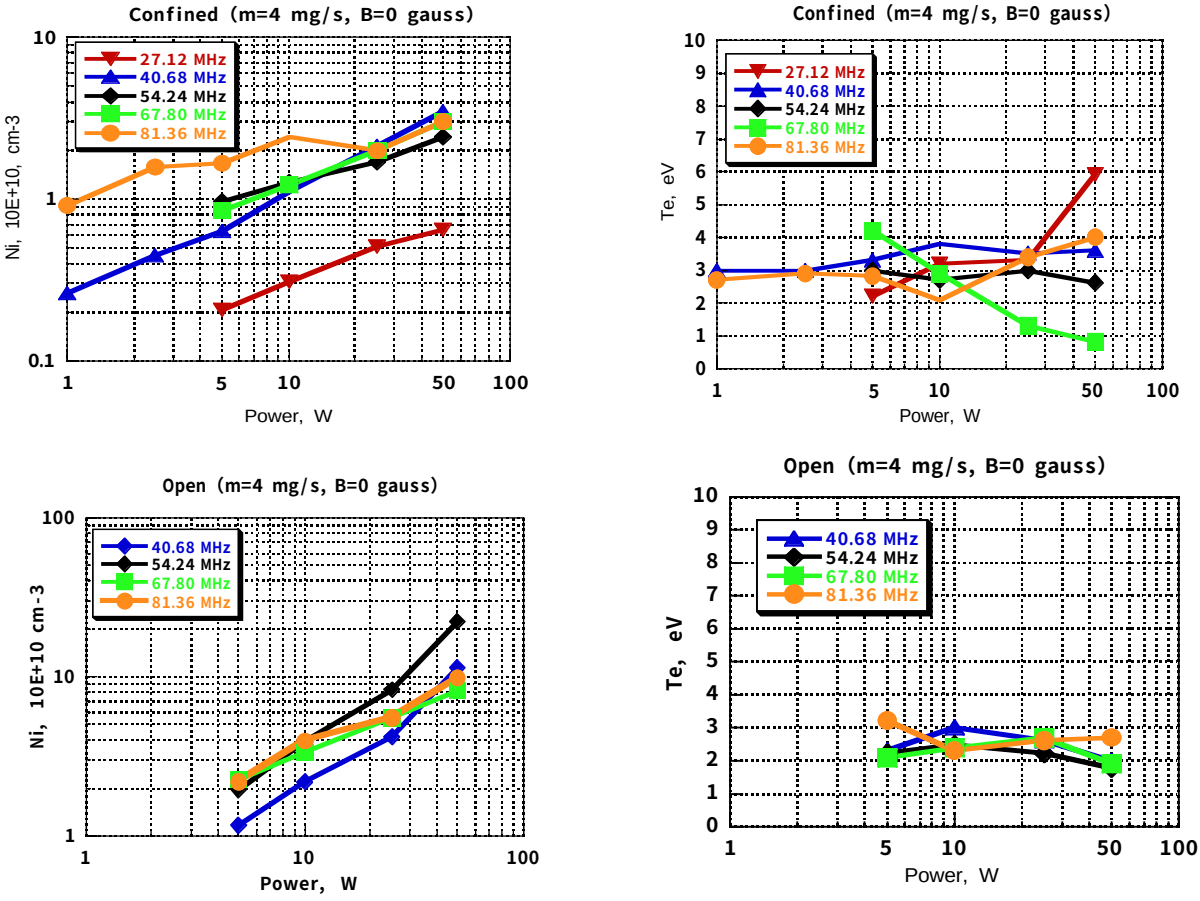

Fig. 11 Plasma density and electron temperature without B- field at Ar flowrate of 4 mg/s vs. RF input power for various RF frequency (Upper: Short (confined) source, Lower: Long (open) source).

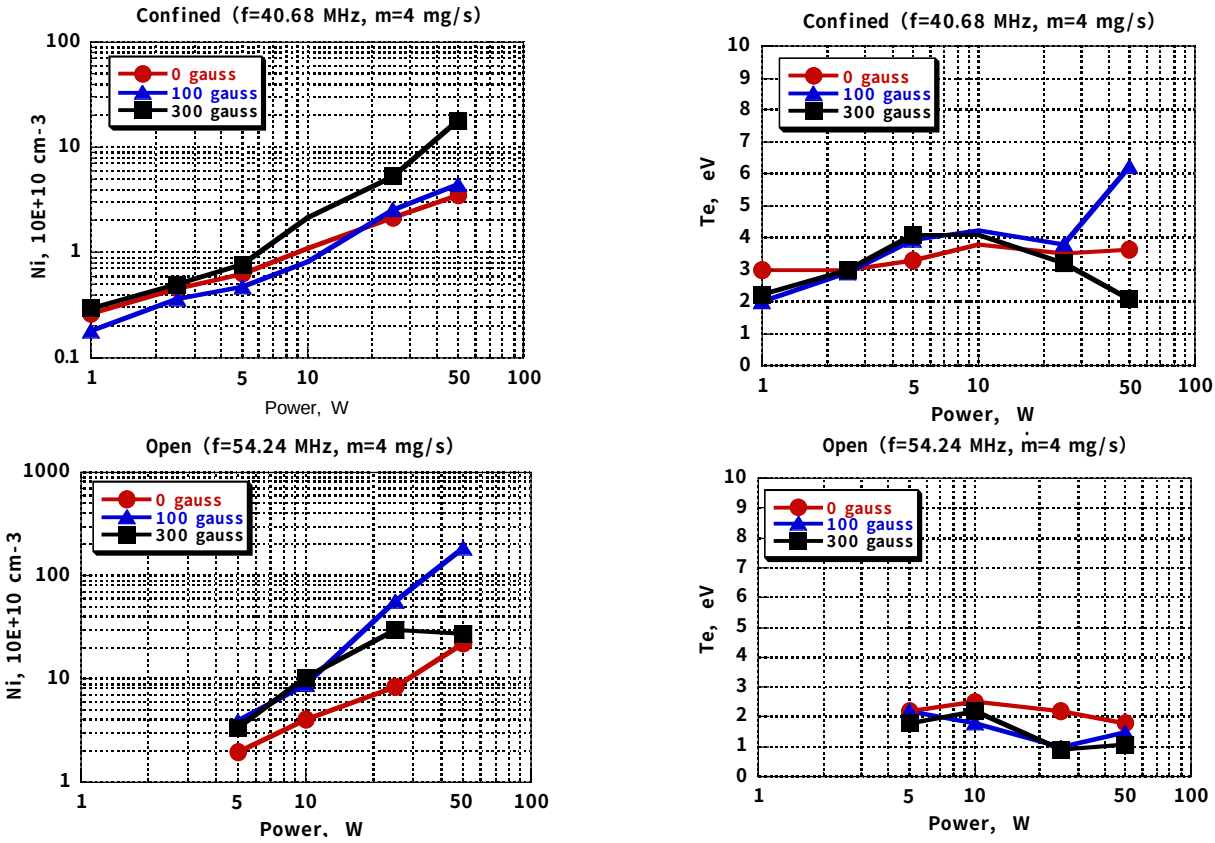

Fig. 12 Plasma density and electron temperature at Ar flowrate of 4 mg/s vs. RF input power for various B-fields (Upper: Short (confined) source, Lower: Long (open) source).

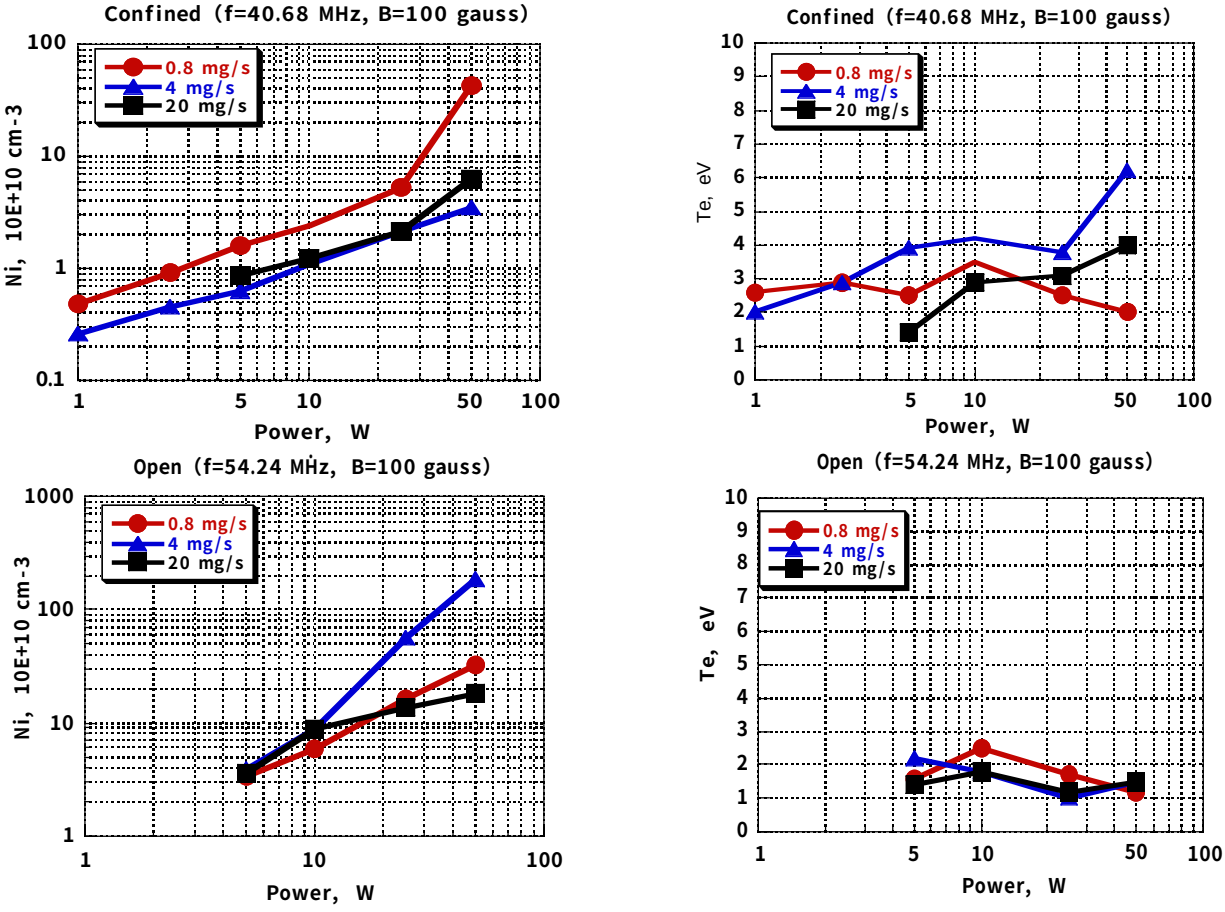

Fig. 13 Plasma density and electron temperature at a B-field of 100 gauss vs. RF input power for various flowrates (Upper: Short (confined) source, Lower: Long (open) source).

observed at 0.8 mg/s under 100 gauss for Short (confined) source in Fig. 12 and the rapid density increase observed at 4 mg/s under 100 gauss for Long (open) source in Fig. 13 is considered as helicon modes.

5. Discussions and Theoretical Prediction

In the analytical prediction the plasma load resistance and profiles of the RF power absorption were evaluated using a model of the source reported as shown in Fig. 14,[14] with specific geometrical parameters similar to experimental conditions described above. Two options were examined, i.e.,Long source of length 15 cm instead of open and Short source of length 4.7 cm, both 2.5 cm in diameter. The computations were performed for Ar pressure of 30 mTorr and electron temperature of 4 eV. The radial plasma profile was assumed to be of parabolic form with edge density equal to 1 % of the center density, n_0.

Figure 15 shows the plasma resistance in the ICP mode, i.e., at zero external magnetic field. One can see that the resistance values are practically equal in both cases. The reason is that the RF power in this mode is absorbed under the antenna in a narrow layer of width equal to the skin size which is smaller than the source size, as seen from Fig. 16. The resistance increases with density but remains at a quite low level even in the range of 10^{12} cm^{-3}. It turns out to be somewhat higher at a higher excitation frequency (see Fig. 15). The increase of the plasma resistance occurs in the helicon mode, i.e., at a finite external magnetic field.

As seen from Fig. 17, for Long source this increase is the most substantial above 200 gauss at an optimal driving frequency about 60 MHz. The resistance is increased even larger and at lower magnetic fields for the small source, as seen from Fig. 18. The main reason for the resistance increase is spreading of the absorption area from the antenna. This effect occurs due to irradiation of waves which is more efficient at higher magnetic fields.[14] Absorption profiles at finite magnetic fields are shown in Fig. 19. In conclusion, an ICP mode of the small source operation seems to be inappropriate from the viewpoint of the high electric efficiency inasmuch as estimated plasma resistance is quite low and thus a fraction of the power absorbed in plasma is comparable with circuitry losses. An economic regime of the source operation

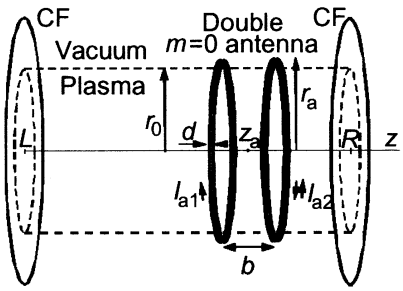

Maxwell Equations
$$c\nabla\times\mathbf{E} = i\omega\mathbf{B}$$
$$c\nabla\times\mathbf{B} = -i\omega\mathbf{D} + 4\pi i_a\delta(r-r_0)$$

Boundary and Joining Conditions
$$\mathbf{E}_t(z=R,\,L)=0$$
$$\{\mathbf{E}_t\}_{r=r_0}=0,\ \{\mathbf{B}_t\}_{r=r_0}=4\pi i_a/c$$

Antenna Current and Fields
$$i_a=\sum i_{k_z}\sin k_z z$$

$k_z = l_z\pi/(R-L),\ l_z = 1,2\ldots l_{z\max}$
$$\mathbf{E}=\sum(\mathbf{E}_\perp\sin k_z z+\hat{\mathbf{z}}E_z\cos k_z z)$$
$$\mathbf{B}=\sum(\mathbf{B}_\perp\cos k_z z+\hat{\mathbf{z}}B_z\sin k_z z)$$

Permittivity Tensor
$$K_1 = 1-\frac{\omega_{pe}^2\gamma_e}{\omega^2\gamma_e^2-\omega_{ce}^2}-\frac{\omega_{pi}^2}{\omega^2\gamma_i},$$
$$K_2=\frac{\omega_{pe}^2\omega_{ce}}{\omega(\omega^2\gamma_e^2-\omega_{ce}^2)},\quad K_3=1+\frac{1}{k_z^2r_{De}^2}\frac{1-w(\xi)}{1-i(\nu_e/\omega\gamma_e)w(\xi)}$$

Collisions and Landau Damping
$$\gamma_{e,i}=1+i(\nu_{e,i}/\omega),\quad \nu_e=\nu_{en}+\nu_{ei},\quad \xi=\omega\gamma_e/k_z v_{Te}$$

Plasma Load Impedance
$$Z_p=-[4\pi^2r_0(R-L)/c]\sum|i_{kz}/I_a|^2\square_\theta(r=r_0)$$

Plasma Density Profile
$$n(r)=n_0-(n_0-n_{edge})(r/r_0)^2$$

Fig. 14 Theoretical model used in the analysis by Shamrai, et al.[15]

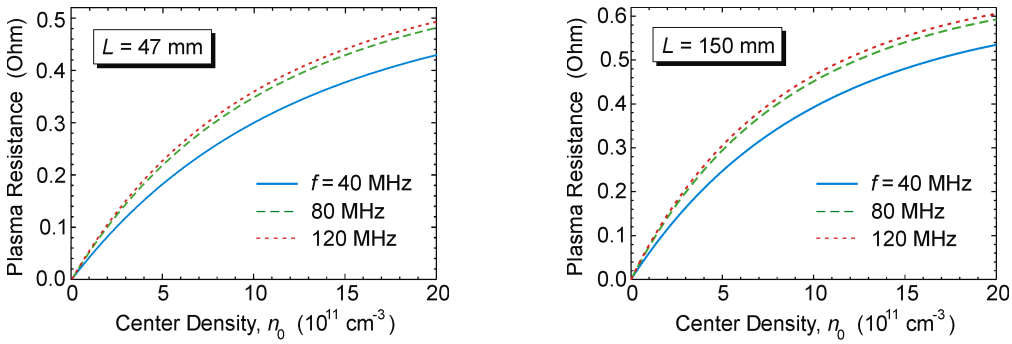

Fig. 15 Dependences of the plasma resistance on density operating in the ICP mode at various frequencies (Left: Short (confined) source, Right: Long (open) source.

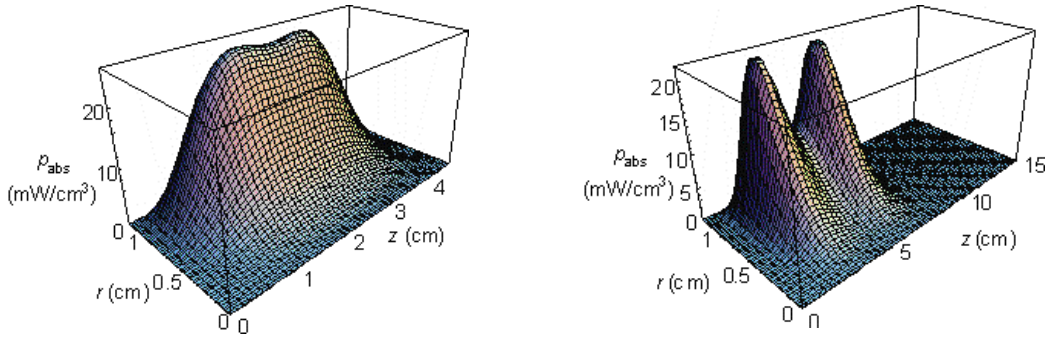

Fig. 16 Absorption profiles for the Short (confined) source and Long (open) source, at zero magnetic field. Plasma density is 2 x 10^{12} cm^{-3} and frequency 60 MHz.

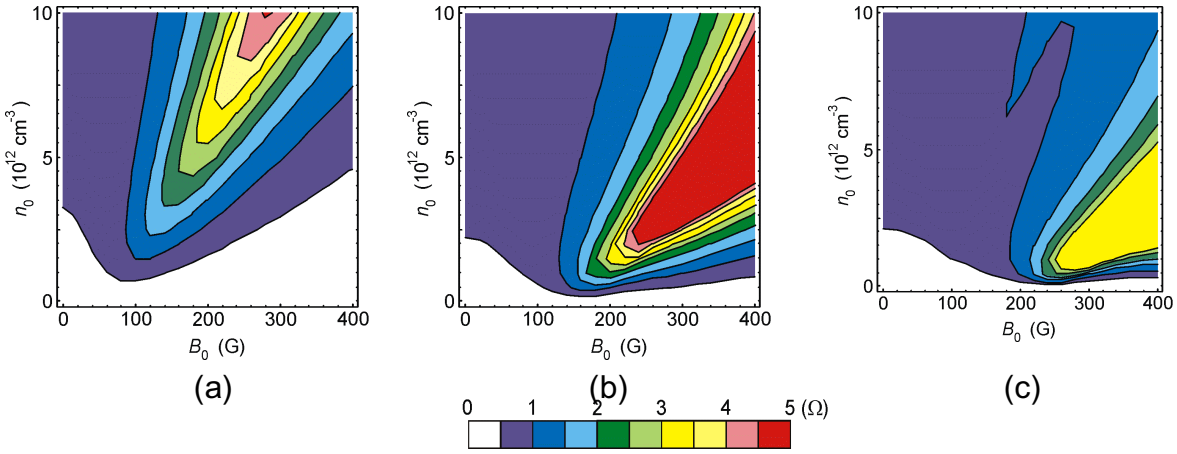

Fig. 17 Contour plots of the plasma resistance for the Short (confined) source as dependent on magnetic field and density, at driving frequencies of (a) 40 MHz, (b) 80 MHz and (c) 120 MHz.

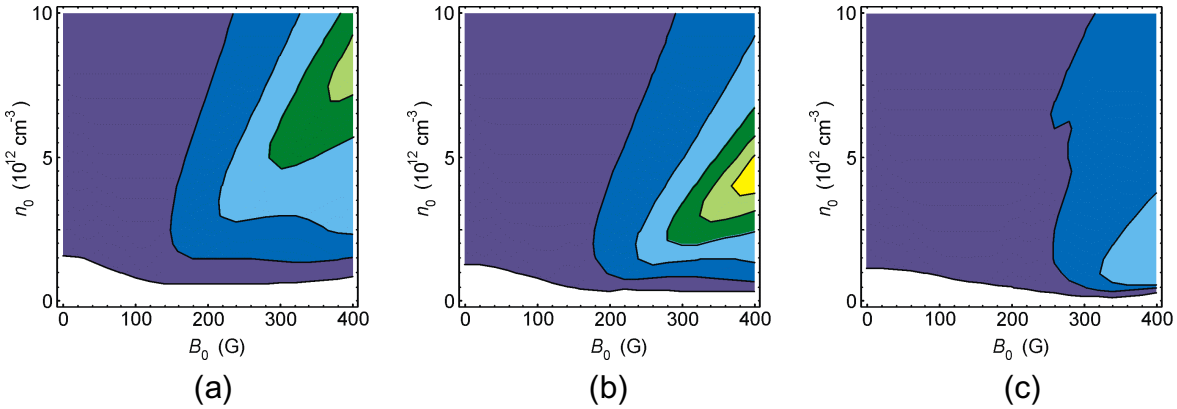

Fig. 18. The same as in Fig. 17 but for the Long (open) source, at frequencies (a) 40 MHz, (b) 60 MHz and (c) 100 MHz.

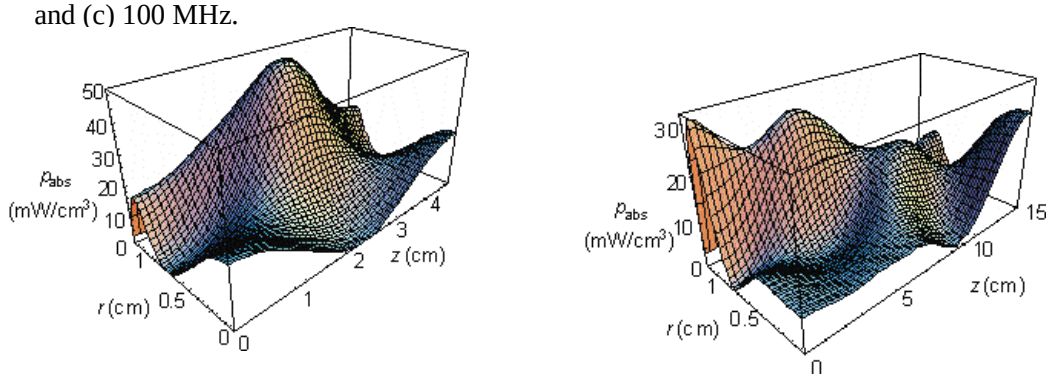

Fig. 19 Absorption profiles for the Short (confined) source at 400 gauss (Left) and for the Long (open-end) source for 100 gauss. Other parameters are the same as in Fig. 16.

can be attained in the helicon mode at magnetic fields of the order of a few hundred gauss. When we think about larger plasma loss in the Short (confined) source, the experimental results do not contradict the theoretical prediction, and large plasma load resistance does not guarantee high density plasma, The higher RF frequencies were not necessarily advantageous in the experiment because smaller mobility of electrons in the ignition phase.

6. Conclusions

For the next generation electric propulsion, a helicon plasma source with rotating electric field acceleration ("Lissajous") of plasma has been proposed and expected as a sort of electrodeless steady-state MPD thruster. Perhaps one of the world smallest helicon plasma source was successfully created for Ar propellant applying a two-loop parallel antenna to a 2.5 cm i.d., 4.7 cm length short confined source and to another long source having an open end at 15cm downstream portion. Appropriate RF frequencies for these ranged from 40 to 80 MHz within 50 W RF input power.. Low frequency of popular 13.56 MHz and high frequency nearly 100 MHz were discarded due to ignition problem. The Long (open) source achieved the plasma density higher than 10^{12} cm^{-3} at 54.24 MHz for of 4 mg/s Ar under the applied magnetic field of 100 gauss. The Short (confined) source indicated an obvious density jump into helicon mode at 40.68 MHz for 0.8 mg/s Ar under the applied magnetic field of 100 gauss. These results encourage the application of the small helicon source as well as the large helicon source to electric propulsions.

References

1. Shinohara, S, "Propagating Wave Characteristics for Plasma Production in Plasma Processing Field", Japanese Journal of Applied Pysics, Vol. 36, Part 1 , No. 7B, July 1997, pp. 4695-4703.
2. Shinohara, S. and Yonekura, K., "Discharge modes and waves structures using loop antennae in a helicon plasma source", Plasma Physics and Controlled Fusion, Vol. 4, 2000, pp. 41-56.
3. Tanikawa, T.,Shinohara, S., Sato, S. and Nakamura, Y., "Large Volume Plasma Production Using Helicon Wave", Bulletin of the American Physical Society, Vol. 47, No. 9 2002, p.47.
4. Shinohara, S. and Tanikawa, T., "Large Helicon Plasma Production by Spiral Antenna", Topic No. 6, XXI International Congress on Phenomena in Ionized Gases, Greifswald, Germany, 2003.
5. Boswell, R., "Very Efficient Plasma Generation by Whistler Waves Near the Lower Hybrid Frequency", Plasma Physics and Controlled Fusion, Vol .26, 1984, p. 1147.
6. Chen, F. F., "Plasma Ionization by Helicon Waves", Plasma Physics and Controlled Fusion, Vol. 33 No. 4 1991, p. 339.
7. Shamrai, K.P., Pavlenko, V.P. and Taranov, V.B., "Excitation, conversion and damping of waves in a helicon plasma source driven by *m = 0* antenna", Plasma Physics and Controlled Fusion, Vol. 39, 1997, p. 505.
8. Chang Diaz, F. R., Squire, J. P., Bengtson, R. D., Breizman, B. N., Baity, F. W. and Carter, M. D., "The Physics and Engineering of the VASIMR Engine", AIAA 2000-3756, 36th AIAA/ASME/SAE/ASEE Joint Propulsion Conference, Hntusville, Alabama, USA, 2000.
9. Ziemba, T. M., Winglee, R. M., Euripides, P. and Slough, J., "Parameterization of the Laboratory Performance of the Mini-Magnetospheric Plasma Propulsion (M2P2) Prototype", IEPC-01-201, 27th International Electric Propulsion Conference, Pasadena, California, USA, 2001.
10. Shamrai, K. P., Aleksandrov, A. F., Bougrov, G. E., Virkov, V. F., Katiukha, V. P., Koh, S. K., Kralkina, E. A., Kirichenko, G. S. and Rukjadze, A. A., "Quasistatic Plasma Sources: Physical Principles, Modelling Experiments, Application Aspects", Journal de Physique IV, Vol. 7, Colloque C4, Supplement au Journal de Physique III, 1997, pp. 365-381.
11. Gilland, J., "The potential for Compact Helicon Wave sources for Electric Propulsion", IEPC-01-0210, 27th International Electric Propulsion Conference, Pasadena, California, USA, 2001.
12. Nakano, T., Toki, K., Ishiyama, A. and Shimizu, Y., "A Feasibility Study of a Low Power Applied-field MPD Arcjet", IEPC-03-92, 28th International Electric Propulsion Conference, Toulous, France, 2003.
13. Kinefuchi, K., Funaki, I., Shimizu, Y. and Toki, K., "Nozzle Shape Effects on Velocity Distribution in an MPD Arcjet", IEPC-03-56, 28th International Electric Propulsion Conference, Toulous, France, 2003.
14. Shamrai, K. P. and Shinohara, S., "Spectral and spatial characterization of a radio frequency power absorption in high pressure helicon plasmas", Physics of Plasmas, Vol. 8 No. 10, 2001, pp. 4659-4674.